Thermoelectric properties of p-type $Bi_{0.5}Sb_{1.5}Te_3$ films on flexible substrate

© Yu.V. Granatkina[1], Z.M. Dashevsky[2]

[1] Baikov Institute of Metallurgy and Materials Science, Russian Academy of Sciences,
119334 Moscow, Russia
[2] OOO RusTec,
109383 Moscow, Russia

E-mail: granat@imet.ac.ru

Received August 18, 2021
Revised August 25, 2021
Accepted August 25, 2021

Bi_2Te_3-based compounds are excellent candidates for the low-temperature thermoelectric application. In the present work, a technology for fabrication of p-$Bi_{0.5}Sb_{1.5}Te_3$ films with high thermoelectric efficiency on a thin flexible polyimide substrate has been developed. The preparation of films was carried out by a flash evaporation method. A systematic study of the transport properties (Hall coefficient, Seebeck coefficient, electrical conductivity, transverse Nernst coefficient) over the entire temperature range of 80−400 K for p-$Bi_{0.5}Sb_{1.5}Te_3$ films has been performed. The power factor (PF) for the $Bi_{0.5}Sb_{1.5}Te_3$ (doped with 0.5 wt% Te) film reached the value of $\sim 30\,\mu W/cm \cdot K^2$, which is among the highest values of the PF reported in the literature to date for a film on a flexible polyimide (amorphous) substrate. The measured thermal diffusivity along the film allowed us to accurately estimate the figure of merit Z for p-$Bi_{0.5}Sb_{1.5}Te_3$ films considering the anisotropic effect of Bi_2Te_3-based materials. A significant enhancement of Z up to $\sim 3.0 \cdot 10^{-3}$ K has been obtained for these films, which is state-of-the-art even compared to bulk materials. This research can provide insight into the fabrication of p-type branch of the film thermoelectric modules (FTEM), which could be a candidate for application in micro-scale thermoelectric generators.

Keywords: p-$Bi_{0.5}Sb_{1.5}Te_3$ film, thin flexible substrate, thermoelectric properties.

DOI: 10.21883/SC.2022.01.53112.05

1. Introduction

Recently the issue of manufacturing the microelectronic transducers with capacity of several microwatt at relatively high voltage for operation of small electric devices and systems has become very relevant [1,2]. Film thermoelectric generator (FTEG) can be perfect power source for such purposes. It can directly generate some electric energy from heat energy. Output capacity of such micro-devices is within 100 nW−10 mW, that is the typical capacity range, generated from the human body surface [3–6]. For making the FTEG with acceptable characteristics the film materials with high thermoelectric characteristics are required [7].

Efficiency of heat conversion into electricity is defined with thermoelectric efficiency Z:

$$Z = \frac{S^2\sigma}{\kappa}, \qquad (1)$$

where S is Seebeck coefficient, σ and κ are electrical conductivity and thermal conductivity, respectively.

Currently Bi_2Te_3 and its alloys are the most effective materials for a range of room temperature [8,9]. Bismuth, stibium and tellur are some of the heaviest elements of the Periodic table, and chemical bonds between them are not particularly strong. Consequently, the elementary cells are large, Brillouin zones and phonons wave vectors are small. This results in naturally low inherent thermal conductivity of lattice even in perfect crystals, where it is limited only with anharmonic phonon-phonon interactions [10]. Hard solution of $Bi_{0.5}Sb_{1.5}Te_3$, alloyed to level of 0.5% by weight of tellur surplus, has maximum value of $ZT \approx 0.9$ for bulk samples [8]. Tellur surplus is used for compensation of the acceptor effect of stibium, appearing as a result of stoichiometry shift [8].

Films based on Bi_2Te_3 were made using methods of combined evaporation, molecular-beam-epitaxy, magnetron sputtering and pulsed laser deposition [11–15]. Structural and microstructural properties of thin films on various types of substrates are well known in the literature [16–20]. However, the high value of Z for films based on Bi_2Te_3, as for bulk crystals ($Z \approx 3 \cdot 10^{-3}\,K^{-1}$) [21–24], was not achieved.

In this study we use method of discrete evaporation, that was developed by Z.M. Dashevsky for making the multicomponent solid solution films [25]. Thin polyimide film with thickness of $\sim 10\,\mu$m was used as substrate. Advantages of polyimide materials as the substrate are in its low thermal conductivity (~ 0.3 W/mK), strength to substrate heat temperature of $T \approx 700$ K and flexibility, that is especially important for development of compact film thermoelectric microgenerators [25].

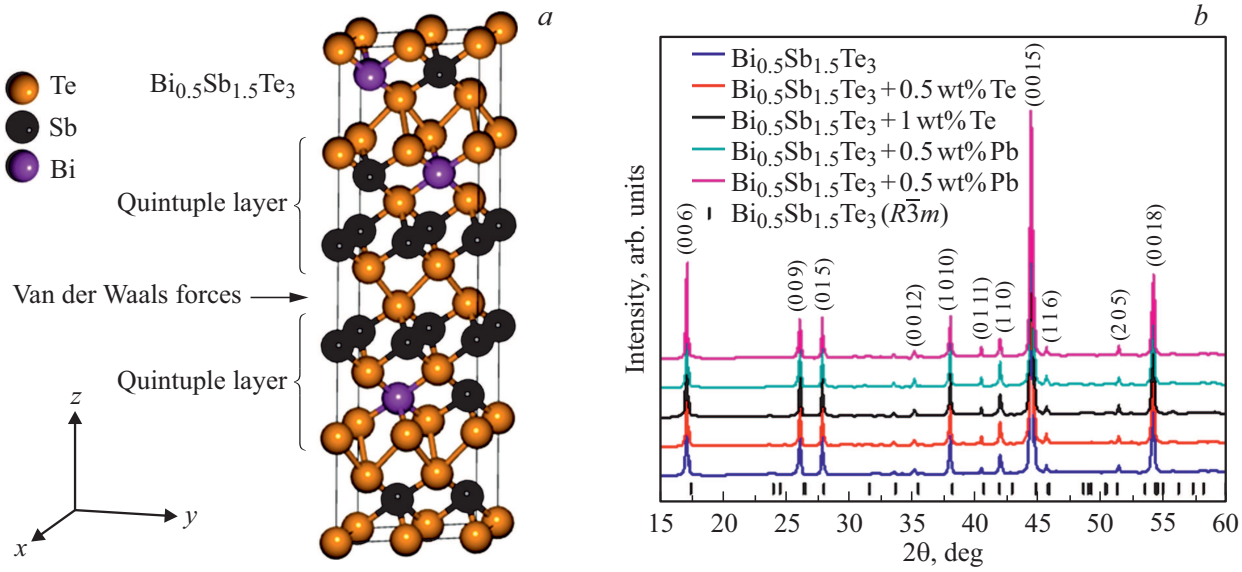

Figure 1. Crystal structure of $Bi_{0.5}Sb_{1.5}Te_3$ (a) and X-ray images of films of $Bi_{0.5}Sb_{1.5}Te_3$ on polyimide substrate (b).

2. Experimental part

Synthesis of materials based on $Bi_{0.5}Sb_{1.5}Te_3$ was performed using direct fusion of components for 10 h at 1073 K in sealed quartz vessel, vacuumized to residual pressure of 10^{-5} Torr. Then the vessel was removed from a furnace and water-cooled. High purity components were used for the synthesis. The resulting ingots were reduced to fine powder in a ball mill under argon atmosphere. Manufacturing of films of $Bi_{0.5}Sb_{1.5}Te_3$ with higher concentration of holes was performed using hyperstoichiometric Pb (0.5–1.0% by mass) by means of the acceptor effect of Pb in compositions based on Bi_2Te_3 [8]. The lower concentration of holes in $Bi_{0.5}Sb_{1.5}Te_3$ was observed by introduction of hyperstoichiometric Te (0.5–1% by mass), which is due to metal vacancies compensation effect [8].

Films of $Bi_{0.5}Sb_{1.5}Te_3$ of p-type of conductivity were deposited using discrete evaporation method [14,25]. Substrate temperature was $T_s = 523$ K, evaporation rate — $V_p \sim 0.1\,\mu$m/min. After the process all films were annealed in the same testing chamber at $T_o = 623$ K for 0.5 h under argon atmosphere at pressure $P = 0.9$ atm.

Structural analysis of films was performed at X-ray diffractometer STOE STADI P (STOE & Cie GmbH, Germany) as per modified scheme of Guinier geometry using transmission mode ($CuK_{\alpha 1}$-radiation, Ge-monochromator (111) of Johann type; $2\theta/\omega$-scanning, angular spacing $15° \le 2\theta \le 60°$). The initial processing of experimental results was performed using PowderCell software packages. The secondary emission electronic images were made using scanning election microscope (HRSEM).

The unique measuring apparatus was used for studying the transport parameters of thin films (Seebeck coefficient S, electrical conductivity σ, Hall coefficient R_H and Nernst–Ettingshausen transversal effect coefficient Q) in a wide range of temperatures 80–400 K [26]. Measuring of Hall effect and Nernst–Ettingshausen transversal effect was performed in static magnetic fields of up to 2 T. Temperature measurements accuracy was 0.1–0.2 K, while magnetic field accuracy — ±3%. Measuring error of Seebeck coefficient and electrical conductivity was 6%. Hall effect was measured with accuracy of 8%, while Nernst–Ettingshausen transversal effect — with accuracy of 10%.

Study of thermal conductivity in films of p-$Bi_{0.5}Sb_{1.5}Te_3$ on polyimide substrate was made using optical method, that is described in detail in [27]. Thermal conductivity measurement error α was $\sim 8\%$. The general heat conductivity was calculated as per formula

$$\kappa = \alpha \rho c_p, \tag{2}$$

where ρ is the monocrystal density, and c_p was evaluated as per Dulong–Petit law.

3. Results and discussion

3.1. Structural properties

Bi_2Te_3 and Sb_2Te_3 constitute the continuous series of solid solutions [8]. Structure of $Bi_{0.5}Sb_{1.5}Te_3$ consists of five layers, that are perpendicular to z axis in hexagonal lattice, as shown in Fig. 1, a.

Quality of studied samples after synthesis and film deposition was evaluated using X-ray structural analysis method. Figure 1, b shows X-ray images for films based on $Bi_{0.5}Sb_{1.5}Te_3$ on amorphous thin polyimide substrate. Sharp and multiple diffraction peaks indicate polycrystalline

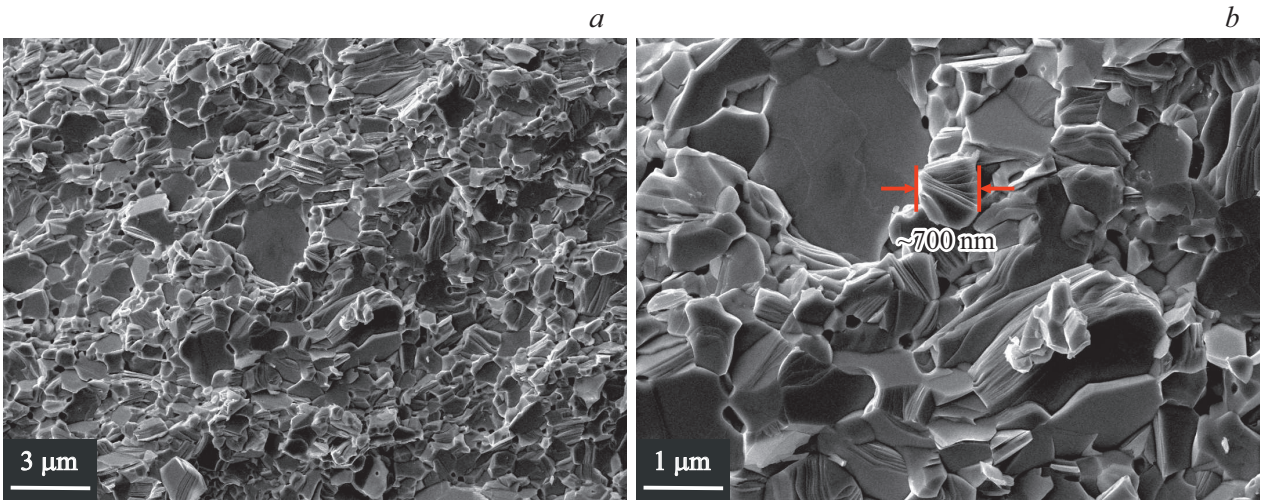

Figure 2. Images in secondary electrons of $Bi_{0.5}Sb_{1.5}Te_3$ film surface on polyimide substrate.

nature of studied samples. Peaks (006) and (0015) are the most intensive, the similar image was observed for films of $Bi_{0.5}Sb_{1.5}Te_3$, prepared using magnetron sputtering method [14]. This indicates the high quality of sample [00l] texture, i.e. all studied films were oriented along substrate plane in direction, perpendicular to crystallographic axis of c of $Bi_{0.5}Sb_{1.5}Te_3$ lattice. Diffractogram of films corresponds to the structure type of $Bi_{0.5}Sb_{1.5}Te_3$ and does not contain foreign peaks, that indicates the single-phase nature of the resulting samples due to small number of doping impurities used in operation.

Figure 2 shows emission images in secondary electrons of $Bi_{0.5}Sb_{1.5}Te_3$ film surface. As shown in Fig. 2, *a*, there are no pores for the studied film. Crystallites surface is well-visible in the high magnification image in Fig. 2, *b*. The image shows formation of platy grains, characteristic for layer structures of the studied solid solution. The average grain size for a film on amorphous substrate is $\sim 700\,\text{nm}$, while the size of the largest grains is up to $\sim 3\,\mu\text{m}$.

3.2. Transport properties

Figure 3 shows dependencies of Hall coefficient R_H (a), Seebeck coefficient S (b), electrical conductivity σ (c) and Nernst–Ettingshausen transversal effect coefficient Q (d) on temperature in a range of 80–400 K for films of p-$Bi_{0.5}Sb_{1.5}Te_3$, additionally alloyed with tellur (donor) or lead (acceptor), with thickness of $(3 \pm 0.5)\,\mu\text{m}$ on polyimide substrate.

For all films the Hall coefficient R_H was positive over the whole studied range of temperatures. For samples of stoichiometric composition the value of R_H, essentially independent of temperature, is characteristic. For samples, alloyed with tellur (donor in this case), the Hall coefficient is slightly reducing with temperature rising.

Figure 3, *b* shows Seebeck coefficient S for films of p-$Bi_{0.5}Sb_{1.5}Te_3$ depending on temperature. Seebeck coefficient for all films has positive values in the specified range of temperatures, that is characteristic for semiconductors with hole-type conductivity. Absolute value of Seebeck coefficient for $Bi_{0.5}Sb_{1.5}Te_3$ with Pb concentration of more than stoichiometric one increases within the studied range of temperature. There is no minority carriers effect due to high concentration of carriers in these films. Seebeck coefficient of stoichiometric film of p-$Bi_{0.5}Sb_{1.5}Te_3$ and film with Te concentration of more than stoichiometric one reaches maximum with temperature rise, and then starts to decrease due to minority carriers impact.

Electrical conductivity of films of p-$Bi_{0.5}Sb_{1.5}Te_3$ decreases with temperature rise as in metal materials (Fig. 3, *c*).

Figure 3, *d* shows temperature dependence of Nernst–Ettingshausen transversal effect coefficient Q in a range of temperatures of 80–400 K for films of p-$Bi_{0.5}Sb_{1.5}Te_3$.

3.3. Thermoelectric properties

The table includes the measured thermoelectric characteristic (Seebeck coefficient S, electrical conductivity σ and heat conductivity κ) at $T = 300\,\text{K}$ for three films of p-$Bi_{0.5}Sb_{1.5}Te_3$ with thickness of $(3 \pm 0.5)\,\mu\text{m}$ on polyimide substrate. Thermoelectric parameters of bulk crystals of p-$Bi_{0.5}Sb_{1.5}Te_3$ from [23,24] are also included in the table. Calculated thermoelectric efficiency Z for film sample with composition of p-$Bi_{0.5}Sb_{1.5}Te_3 + 0.5\%\,\text{Te}$ reached value of $Z \approx 3.0 \cdot 10^{-3}\,\text{K}^{-1}$ at $T = 300\,\text{K}$, that is almost equal to value of Z for bulk samples of p-$Bi_{0.5}Sb_{1.5}Te_3$.

Figure 4 shows power factor PF $(S^2\sigma)$ for films of p-$Bi_{0.5}Sb_{1.5}Te_3$. Samples with Te concentration of more than stoichiometric one have high values of power factor, up to $30\,\mu\text{W/cm} \cdot \text{K}^2$, due to optimum position of Fermi

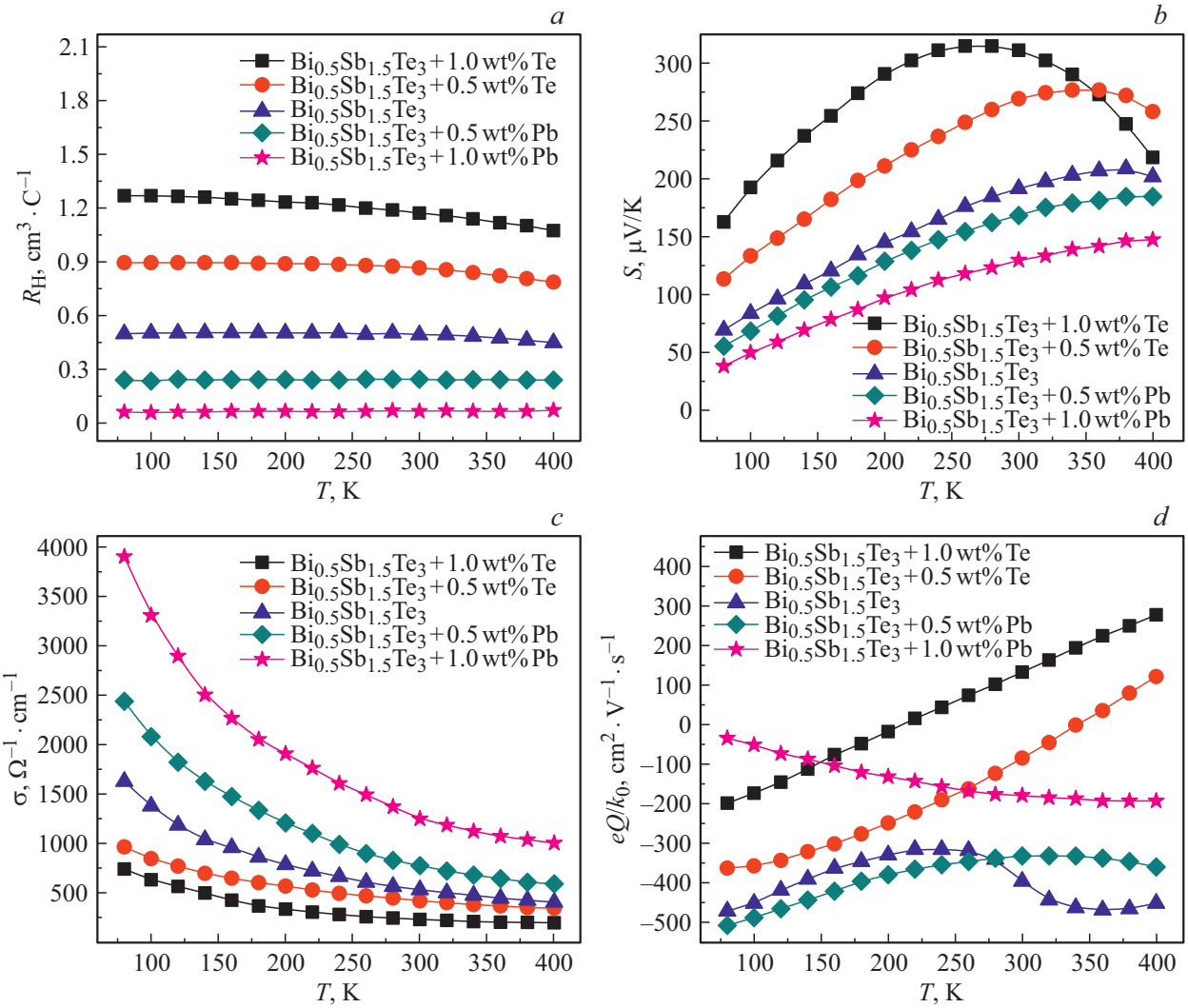

Figure 3. Temperature dependencies of Hall coefficient R_H (*a*), Seebeck coefficient S (*b*), electrical conductivity σ (*c*) and Nernst–Ettingshausen transversal effect coefficient Q (*d*) for films of p-$Bi_{0.5}Sb_{1.5}Te_3$ of various composition.

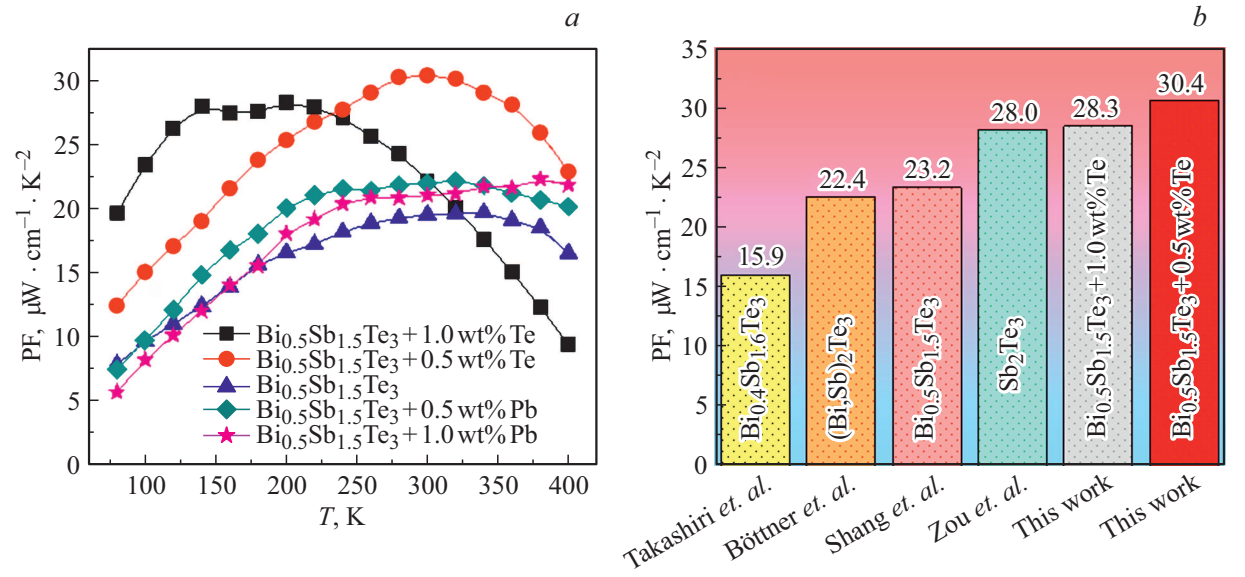

Figure 4. Temperature dependencies of power factor PF ($S^2\sigma$) for films of p-$Bi_{0.5}Sb_{1.5}Te_3$ of various composition (*a*) and comparison of power factor PF for films of p-$Bi_{0.5}Sb_{1.5}Te_3$ with data from studies [14,20,28,29] (*b*).

Thermoelectric properties of films on polyimide substrate and bulk crystals of p-$Bi_{0.5}Sb_{1.5}Te_3$ at $T = 300\,K$

Composition	Sample type	S, $\mu V/K$	σ, $Ohm^{-1} \cdot cm^{-1}$	κ, $W/m \cdot K$	$Z \cdot 10^3$, K^{-1}	Reference
$Bi_{0.5}Sb_{1.5}Te + 1.0\%\,Te$	film	310	230	9.3	2.4	
$Bi_{0.5}Sb_{1.5}Te + 0.5\%\,Te$	film	270	420	10.0	3.0	
$Bi_{0.5}Sb_{1.5}Te + 0.5\%\,Pb$	film	170	775	11.7	1.9	
$Bi_{0.5}Sb_{1.5}Te$	bulk	200	1150	15.5	3.0	[23]
$Bi_{0.5}Sb_{1.5}Te$	bulk	205	1020	14.5	2.9	[24]

level (close to valence band top [7]). The average value of power factor in temperature range of 200−400 K for film of p-$Bi_{0.5}Sb_{1.5}Te_3 + 0.5\%\,Te$ is $\sim 25\,\mu W/cm \cdot K^2$.

4. Conclusion

Films based on $Bi_{0.5}Sb_{1.5}Te_3$ p-type of conductivity with optimum charge carrier concentration were made using discrete evaporation method. Process parameters of manufacturing the films of p-$Bi_{0.5}Sb_{1.5}Te_3$ on thin flexible (polyimide) substrate were optimized.

Systematic study of transport properties of films of p-$Bi_{0.5}Sb_{1.5}Te_3$ with various composition was performed; Hall coefficient R_H, Seebeck coefficient S, electrical conductivity σ, Nernst−Ettingshausen transversal effect coefficient Q were measured within temperature range of 80−400 K.

Power coefficient PF ($S^2\sigma$) for a film of p-$Bi_{0.5}Sb_{1.5}Te_3$, additionally alloyed with 0.5% Te by mass, is $\sim 30\,\mu W/cm \cdot K^2$ at $T = 300\,K$.

Thermal conductivity along film of p-$Bi_{0.5}Sb_{1.5}Te_3$ was measured, that allowed to evaluate thermoelectric efficiency Z. The observed value of $Z \approx 3.0 \cdot 10^{-3}\,K^{-1}$ at $T = 300\,K$ for film of $Bi_{0.5}Sb_{1.5}Te_3 + 0.5\%\,Te$ is one of the maximum values of Z for films of p-$Bi_{0.5}Sb_{1.5}Te_3$ on amorphous substrate.

Significant increase of thermoelectric characteristic of films of p-$Bi_{0.5}Sb_{1.5}Te_3$ on thin flexible substrate opens new possibilities for development of film thermoelectric transducers [30].

Conflict of interest

The authors declare that they have no conflict of interest.

References

[1] A.P. Goncalves, C. Godart. In: *New Materials for Thermoelectric Applications: Theory and Experiment*, ed. by V. Zlatic, A. Hewson (Springer, N.Y., 2013) p. 1.

[2] D.M. Rowe. *Thermoelectric Handbook: Macro to Nano* (CRC Press, Boca Raton, 2005).

[3] K. Tappura, K. Jaakkola. Proceedings, **2**, 779 (2018).

[4] Krisina T. Settaluri, Hsinyi Lo, Rajeev J. Ram. J. Electron. Mater., **41**, 984 (2012).

[5] R. Venkatasubramanian, E. Siivola, T. Colpitts, B. O'Quinn. Nature, **413**, 597 (2001).

[6] P. Fan, Z. Zheng, Z. Cai, T. Chen, R. Lin. Appl. Phys. Lett., **102**, 033904 (2013).

[7] Z. Dashevsky, S. Skipidarov. In: *Novel Thermoelectric materials and Device Design Concepts*, ed. by M. Nikitin, S. Skipidarov (Springer, N.Y., 2019) p. 3.

[8] B.M. Gol'cman, V.A. Kudinov, I.A. Smirnov. *Poluprovodnikovye termoelektricheskie materialy na osnove Bi_2Te_3* (M., Nauka, 1972) (in Russian).

[9] J. Herremans, B. Wiendliocha. In: *Aspect of Thermoelectricity*, ed. by C. Uher (CRS Press, Boca Raton, 2016) p. 39.

[10] O. Ben-Yehuda, R. Shuker, Y. Gelbstein, Z. Dashevsky, M.P. Dariel. J. Appl. Phys., **101**, 113707 (2007).

[11] L.M. Goncalves, C. Couto, P. Alpuim, A.G. Rolo, F. Völklein, J.H. Correia. Thin Sol. Films, **518**, 2816 (2010).

[12] X. Duansides, Y. Jiang. Appl. Surf. Sci., **256**, 7365 (2010).

[13] L.W. da Silva, M. Kaviany, C. Uher. J. Appl. Phys., **97**, 114903 (2005).

[14] M. Takashiri, T. Shirakawa, K. Miyazaki, H. Tsukamoto. Sensors Actuators A Phys., **138**, 329 (2007).

[15] G. Wang, L. Endicott, C. Uher. Sci. Adv. Mater., **3**, 73 (2011).

[16] E. Symeou, M. Pervolaraki, C.N. Mihailescu, G.I. Athanasopoulos, C. Papageorgiou, T. Kyratsi, J. Giapintzakis. Appl. Surf. Sci., **336**, 138 (2015).

[17] P. Fan, Z.-H. Zheng, Z.-K. Cai, T.-B Chen, P.-J. Liu, X.-M. Cai, D.-P. Zhang, G.-X. Liang, J.-T. Luo. Appl. Phys. Lett., **102**, 033904 (2013).

[18] D. Bourgault, C.G. Garampon, N. Caillault, L. Carbone, J.A. Aymami. Thin Sol. Films, **516**, 8579 (2008).

[19] H. Obara, S. Higomo, M. Ohta, A. Yamoroto, K. Ueno, T. Iida. Jpn. J. Appl. Phys., **48**, 085506 (2009).

[20] H. Zou, D.M. Rowe, S.G.K. Williams. Thin Sol. Films, **408**, 270 (2002).

[21] H.-J. Wu, W.-T. Yen. Acta Mater., **157**, 33 (2018).

[22] R. Deng, X. Su,, S. Hao, S. Zheng, M. Zhang, H. Xie, W. Liu, Y. Yan, V. Wolverton, C. Uher, M.G. Kanatzidis, X. Tang. Energy Environ. Sci., **6**, 1520 (2018).

[23] Z.M. Dashevsky, P.P. Konstantinov, S.Ya. Skipidarov. Semiconductors, **53**, 861 (2019).

[24] L.D. Ivanova, L.I. Petrova, Ju.V. Granatkina, V.B. Sokolov, S.Ja. Skipidarov, N.I. Duvankov. Inorg. Mater., **44**, 687 (2008).

[25] B.M. Gol'cman. Z.M. Dashevsky. V.M. Kajdanov. *Plenochnye termoelementy: fizika i primenenie* (M., Nauka, 1985) (in Russian).
[26] B. Dzundza, L. Nykyruy, T. Parashchuk, E. Ivakin, Y. Yavorsky, L. Chernyak, Z. Dashevsky. Physica B, **588**, 412178 (2020).
[27] E.V. Ivakin, I.G. Kisialiou, L.I. Nykyruy, Y.S. Yavorskyy. Semiconductors, **52**, 1691 (2018).
[28] H. Shang, C. Dun, Y. Deng, T. Li, Z. Gao, L. Xiao, H. Gu, D.J. Singh, Z. Ren, F. Ding. J. Mater. Chem. A, **8**, 4552 (2020).
[29] H. Bottner, J. Nunus, A. Gavrikov, G. Kühner, M. Jägle, C. Künzel, D. Eberhard, G. Plescher, A. Schubert, K.-H. Schlereth. J. Microelectromech. Syst., **13** (3), 414 (2004).
[30] M. Maksymuk, T. Parashchuk, B. Dzundza, L. Nykyruy, L. Chernyak, Z. Dashevsky. J. Mater. Today Energy, **21**, 100753 (2021).